Grid Synchronization of Brushless Doubly Fed Asynchronous Generators in Wind Power Systems

R. Carlson, *Senior Member, IEEE*, and H. Voltolini, Member*, IEEE*

***Abstract*-- The vector control of the Brushless Doubly Fed Induction Generator (BDFIG) was implemented in Matlab/Simulink/SymPowerSystems using a rotating reference frame fixed on the power winding flux. The control algorithms of the grid-side and control-side converters can regulate the active and reactive power independently. The measure of the power winding flux angle, realized using a PLL, showed good performance during the system startup and has demonstrated a robust behavior under noisy voltage and current signals. A synchronization strategy is proposed that acts on the control-side converter current control loops to ensure the conditions for a smooth connection. Soft and fast synchronization is achieved at the minimum rotating speed. To validate the simulated results an experimental setup with a Doubly Fed Induction Generator with brushes was tested with the same control strategy and the experimental results showed coherent with the simulated ones.**

***Index Terms*-- Brushless, induction generator and synchronization.**

I. Nomenclature

θ_e…	Grid voltage space vector position
θ_p…	Power winding flux position
λ_s…	Power winding vector space flux
λ_{qp}…	q-axis power winding flux
λ_{dp}…	d-axis power winding flux
ω_r…	Rotor speed
P_e…	Grid active power
Q_e…	Grid reactive power
v_{qe}…	q-axis grid voltage
v_{de}…	d-axis grid voltage
i_{qe}…	q-axis grid current
i_{de}…	d-axis grid current
L…	Grid converter line choke inductance
R…	Grid converter line choke resistance
V_{q1}…	q-axis AC-side grid converter voltage
V_{d1}…	d-axis AC-side grid converter voltage
V_e…	Grid voltage space vector

R. Carlson is with Universidade Federal de Santa Catarina, Florianopolis, SC 88058-500 Brazil (e-mail: rcarlson@ieee.org).

H. Voltolini is with Universidade Tecnologica Federal do Paraná,Ponta Grossa, PR 84016-210 Brazil (e-mail: hvoltolini@utfpr.edu.br).

II. Introduction

DOUBLY-FED induction generators (DFIG) with a wound rotor are used as variable speed electric generator especially in wind power generators systems [1]. This type of generator is controlled by power converters with reduced power rating when compared with the machine electrical power output. The stator winding is connected to the electrical grid and the rotor winding is connected to a bi-directional static power converter through slip-rings. The presence of slip rings reduces the lifetime of the machine and increases the maintenance costs.

An alternative to overcome this drawback is the brushless doubly-fed induction generator (BDFIG) [2,3]. The BDFIG has its origins in the technology of cascade induction machines and consists of two three-phase windings with different number of pairs of poles in the stator and a special rotor cage. The stator power and control windings are connected to the three phase power grid; the power winding is connected directly while the control winding is connected through a bi-directional static power converter. A simplified block-diagram of the BDFIG complete system is presented on Fig. 1.

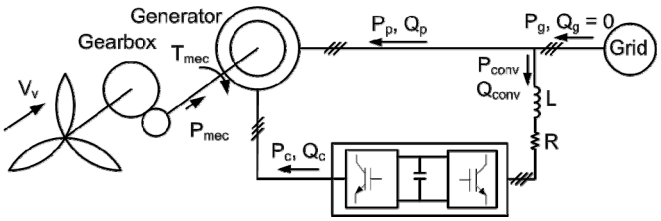

Fig. 1. Representation of the power flow in the system using a 'motor' convention.

Very few references exist on the synchronization process of doubly-fed induction generators [4-7] and none concerning the BDFIG. A method to synchronize the BDFIG to the grid is presented here that exploits the large capacity of the microprocessors that already control the PWM converters.

This paper presents an analysis of the BDFIG's vector control based on simulated results with Matlab/Simulink/ SymPowerSystem. Dynamic results of the control algorithm and grid synchronization process are presented.

III. THE STATIC POWER CONVERTERS

A. The grid-side converter

The grid-side PWM voltage fed converter is connected to the grid through three single-phase chokes. With this configuration it is possible to operate using boost mode and have attractive features as constant DC bus voltage, low harmonic distortion of grid current, bidirectional power flow and adjustable power factor. The main objective of the grid-side converter is to keep the DC-link voltage constant regardless the magnitude and direction of the control winding power. The grid-side converter control, shown in Fig. 2, is based on the dq voltage equations of the grid-reactance-converter system expressed as:

$$\left.\begin{aligned} v_{qe} &= Ri_{qe} + L\frac{di_{qe}}{dt} + \omega_e L i_{de} + v_{ql} \\ v_{de} &= Ri_{de} + L\frac{di_{de}}{dt} - \omega_e L i_{qe} + v_{dl} \end{aligned}\right\} \quad (1)$$

where L and R are the inductance and resistance of the chokes, respectively, v_{qe}, v_{de}, i_{qe}, i_{de} are the electrical grid voltages and currents, v_{ql} and v_{dl} are the AC side voltages of the converter all in the dq reference frame and ω_e is the angular frequency of the electrical grid. The vector control approach is used, with a reference frame oriented along the grid voltage vector (V_e) position, such that $v_{de}=V_e$ and $v_{qe}=0$. This allows independent control of the active and reactive power through i_{de} and i_{qe}, respectively according to following equations:

$$\left.\begin{aligned} P_e &= \frac{3}{2}V_e i_{de} \\ Q_e &= -\frac{3}{2}V_e i_{qe} \end{aligned}\right\} \quad (2)$$

The DC link voltage can be controlled for the active power flow between the two converters above the peak value of the grid voltage. Fig. 2 shows the scheme of the grid-side converter and its controls as simulated in Matlab/Simulink/SimPower Systems.

B. The control-side converter

The vector control of the control-side converter is represented in block diagram in Fig. 3. The control of the reactive power is realized by acting over the control winding current i_{dc}. The reference current is given by a PI controller that adjusts the reactive power to a desired amount (e.g. Q_p^*). Similarly, the control of the active power is realized by acting over the control winding current i_{qc}. There are three possible situations for defining the current reference in this case. Two of them require a PI controller and correspond to the two speed limits: the maximum and minimum rotating speed. The third one corresponds to track the maximum turbine power for each wind speed.

IV. POWER WINDING FLUX ESTIMATION

The aim of the control-side converter is to impose a current to the control winding and to control independently the active and reactive power in the power winding.

After the acquisition, the power winding abc voltages and currents are transformed into a stationary αβ coordinate system. The axis α is aligned with the line-to-neutral voltage V_{an}. Then, the αβ power winding voltages and currents are calculated as:

$$\left.\begin{aligned} V_{\alpha p} &= \frac{1}{3}\left(V_{abp} - V_{cap}\right) \\ V_{\beta p} &= -\frac{1}{\sqrt{3}}\left(V_{abp} + V_{cap}\right) \end{aligned}\right\} \quad (3)$$

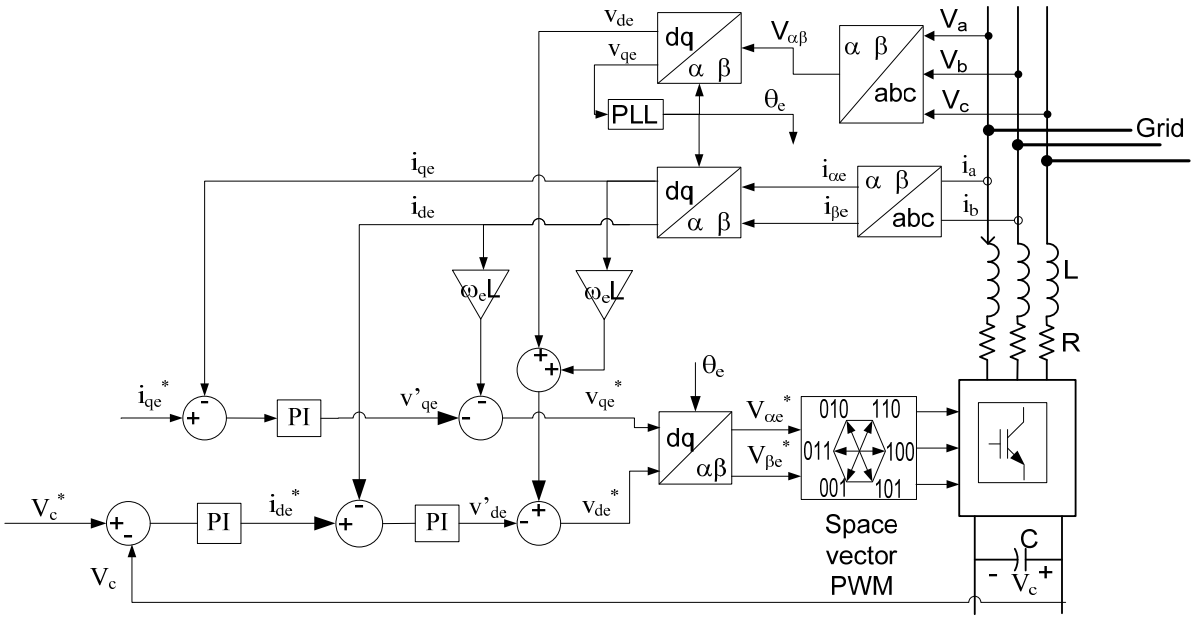

Fig. 2. Control system for the grid-side converter.

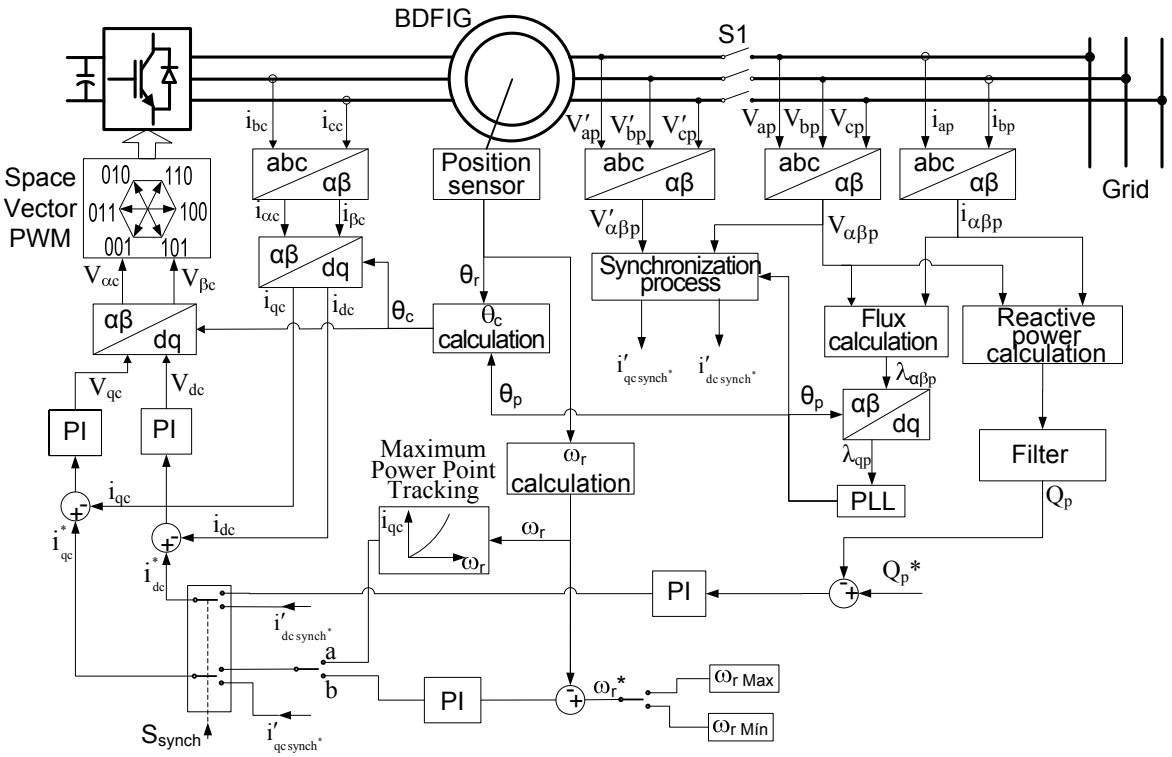

Fig. 3. Control-side converter control strategy block diagram.

$$\left.\begin{aligned} i_{\alpha p} &= i_{ap} \\ i_{\beta p} &= \frac{1}{\sqrt{3}}\left(i_{ap} + 2i_{bp}\right) \end{aligned}\right\} \quad (4)$$

The power winding flux is calculated in the stationary αβ and rotating dq axes as:

$$\left.\begin{aligned} \lambda_{\alpha p} &= \int\left(V_{\alpha p} - r_p i_{\alpha p}\right) dt \\ \lambda_{\beta p} &= \int\left(V_{\beta p} - r_p i_{\beta p}\right) dt \end{aligned}\right\} \quad (5)$$

$$\left.\begin{aligned} \lambda_{dp} &= \lambda_{\alpha p}\cos\left(\theta_p\right) + \lambda_{\beta p}\sin\left(\theta_p\right) \\ \lambda_{qp} &= -\lambda_{\alpha p}\sin\left(\theta_p\right) + \lambda_{\beta p}\cos\left(\theta_p\right) \end{aligned}\right\} \quad (6)$$

Fig. 4 shows the block diagram of the αβ/dq transformation and a phase locked loop (PLL) used for power winding flux angle estimation. In resume, the PLL provides the power winding flux angle such that the d-axis is aligned with total power winding flux λ_p, i.e., $\lambda_{dp}=\lambda_p$ and $\lambda_{qp}=0$. In order to set the initial condition of integration block the constant ω_e (angular grid frequency) is added after the PI controller [8].

The dynamic performance of the PLL during the startup of the system is shown in Fig. 5. This result shows that, at the startup system, the flux position operating point is reached in approximately 0.1s. This flux angle estimator strategy has demonstrated a good performance even in the presence of noise in the voltage and current acquisition.

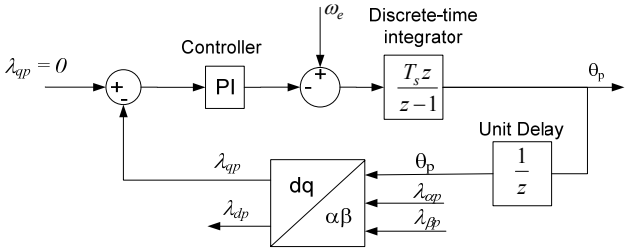

Fig. 4. PLL power winding flux angle estimation.

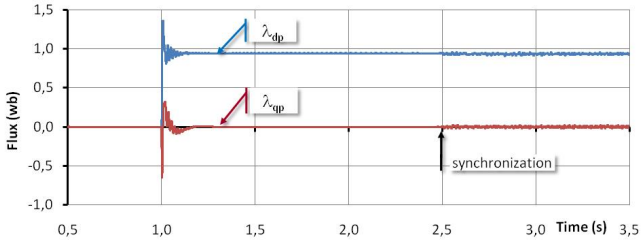

Fig. 5. Estimated dq power winding flux dynamics.

V. SYNCHRONIZATION TO THE GRID STRATEGY

The grid connection is realized when the machine speed reaches the minimum operating value. A soft connection of the generator to the grid is obtained when the phase, frequency and amplitude of the power winding and grid voltages are equal before the switch S1 of Fig. 2 is closed.

The block diagram in Fig. 6 shows how the synchronization of the power winding and grid voltages algorithm was implemented.

To start synchronizing the generator with the grid, the control winding is fed by the back-to-back converters to create a power winding flux and induced voltages. The power winding voltages V'_{abp}, V'_{cap} and the grid voltages V_{abp} and V_{cap} are acquired using similar procedures. With the angle θp, obtained from the PLL, the transformation αβ/dq is applied to both grid and power winding voltages. The grid voltages V_{dp} and V_{qp} are compared to the power winding voltages V'_{dp} and V'_{qp}. The resulting error is processed by the PI controller that acts over the control winding idc and iqc current control loops. As the angle used in the grid and power winding αβ/dq voltages transformation is the same, equal V_{dp} and V'_{dp} values and equal V_{qp} and V'_{qp} values imply equal phase, frequency and amplitude of the grid and power winding voltages. In other words, when the error signals of the dq grid and power winding voltages reaches a small defined value; the synchronism is attained and the system is ready for connection. At this moment a signal is sent by the software to turn on switch S1.

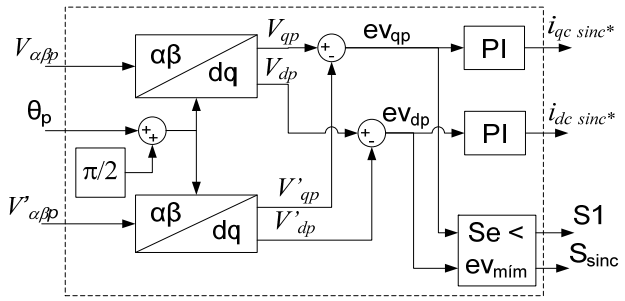

Fig. 6. Block diagram of the synchronization controller.

Fig. 7 shows the simulated results of a synchronization process, t1 and t2 define the initial and the final instants of the process, here they are t1=2.38 s and t2 = 2.45 s.

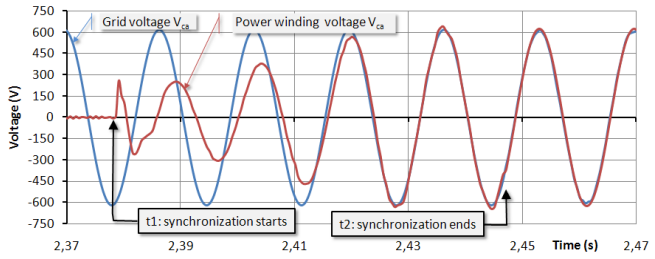

Fig. 7. Simulated results: power winding and grid voltages during the synchronization

The quality of the synchronization procedure can be evaluated examining the phase 'a' currents in both the power and the control windings presented in Fig. 8. No severe transient is observed on those currents.

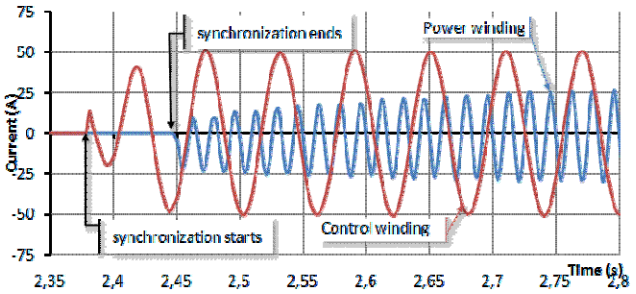

Fig. 8. Simulated results: Power and control winding phase 'a' currents during the synchronization process.

VI. Experimental Results on a Brush DFIG System

In order to verify the control and synchronization strategy here proposed, an experimental bench based on a wound rotor induction machine was set-up (brush DFIG). The same strategy and components were used in this test bench.

Fig. (9) shows the grid and stator voltages during the synchronization process as well as the rotor currents.

The experimental dq voltages of Fig. 9 are shown in Fig. 10 during the synchronization process. In this figure, t1 corresponds to the start of the synchronization procedure. At time t2 the grid side and the stator side voltages amplitude, phase and frequency are sufficiently close and the order is given to switch S1 to close. However, there is a time delay between the instant the order to close is send (t2) and the instant the switch is effectively closed (t3).

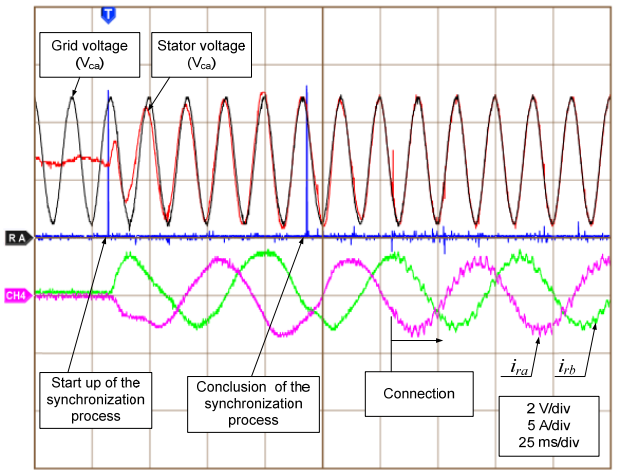

Fig. 9. Experimental results of a brush DFIG - stator and grid voltages, i_{ra} and i_{rb} rotor currents during the synchronization process.

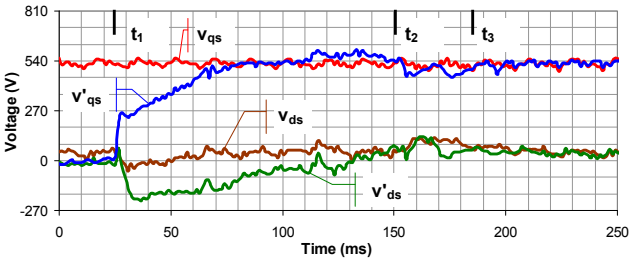

Fig. (10): Experimental dq grid and stator voltages of a brush DFIG during the synchronization process.

VII. Conclusions

In this paper the vector control of the BDFIG using a rotating reference frame fixed on the power winding flux was implemented in Matlab/Simulink/SymPowerSystems. The simulations of the PLL in order to measure the power winding flux angle show good performance during the system startup and its implementation on an experimental DFIG setup has demonstrated a robust behavior under noisy voltage and current signals.

The proposed synchronization process showed to be fast and smooth. Matching the amplitude, frequency and phase of the power windings and grid voltages it assures the conditions for the connection by acting over the control windings current control loops.

VIII. References

[1] R. Pena, J.C. Clare, G.M Asher, "Doubly fed induction generator using back-to-back PWM converter and its application to variable-Speed wind-energy generation." *IEE Proc.-Electr. Power Appl.*, Vol. 143, No. 3, May 1996.

[2] H. Voltolini, R. Carlson, F. Runcos, N. Sadowskim P. Kuo-Peng, "Performance and Vibration Analysis of a 75 kW Brushless Double-Fed Induction Generator Prototype." in *Proc. IEEE/IAS 41st Annual Meeting*, Florida, EUA, October 8 - 12, 2006.

[3] R. Carlson, H. Voltolini, F. Runcos, P. Kuo-Peng, "A performance Comparison Between Brush and Brushless Doubly FED Asynchronous Generators for Wind Power Systems." In *Proc. International Conference on Renewable Energies and Power Quality* - Palma de Mallorca/Espanha, v.1, p. 1-5, 2006.

[4] Y. Tang and L. Xu, "Flexible active and reactive power control strategy for a variable speed constant frequency generating system," *in IEEE Trans. Power Electron.*, vol. 10, no. 4, pp. 472–478, Jul. 1995.

[5] S. Peresada, A. Tilli, A. Tonielli, "Indirect stator flux-oriented output feedback control of a doubly fed induction machina", *in IEEE Transactions on Control Systems Technology*, vol. 11, no. 6, pp. 875-888, November 2003.

[6] G. Yuan; J. Chai; Y. Li, "Vector control and synchronization of doubly fed induction wind generator system", *in IPEMC 2004*, Volume 2, 14-16 Aug. 2004 pp. 886 - 890. August 14-16, 2004, Xi'an, China.

[7] A.G. Abo-Khalil, D-C Lee, S-H Lee, "Grid connection of doubly-fed induction generators in wind energy conversion system", *in IPEMC 2006*, Vol. 3, 14-16 Aug. 2006, pp. 1 - 5. August 14-16, 2006, Xi'an, China.

[8] V. Kaura, V. Blasko, "Operation of a Phase Locked Loop System under distorted Utility Conditions", *in IEEE Transactions on Industry Applications*, Vol. 33, n. 1, pp. 58-63, January/February 1997.

[9]

IX. Biographies

Renato Carlson (SM'91) was born in Porto Alegre, Brazil, on July 31, 1943. He received the B.C.E.E. degree from the Federal University of Rio Grande do Sul, Porto Alegre, Brazil, in 1969, the M.S.E.E. degree from the Federal University of Santa Catarina, Brazil, in 1973, and the D.Eng. degree from the University Paul Sabatier, Toulouse, France, in 1977. In 1970, he joined the staff of the Electrical Engineering Department, Federal University of Santa Catarina, Brazil, where he has been a Professor of electrical engineering until 1998. He has been Vice-President for Graduate Studies and Research at this university from 1996 up to 1998 when he retired. From 1989 to 1990, he was with the Laboratoire d'Electrotechnique et d'Electronique de Puissance of the Institut National Polytechnique de Toulouse, France, for a sabbatical year, obtaining at this time the Diplôme d'Habilitation à Diriger des Recherches. Although he is retired from the University he maintains research and consultancy activities in the area of electrical machines and drives.

Hélio Voltolini was born in Nova Trento, Santa Catarina, Brazil, on November 13, 1964. He received the B.C.E.E. degree from the Federal University of Santa Catarina, Florianópolis, Brazil, in 1990, and the M.S.E.E. and Doctoral degrees from the same University in 1995 and 2007, respectively. Since 1996 he joined the Electronic Department of the Federal Technological University of Parana – Brazil as Professor. His major field of study is electrical machines, adjustable speed drives, power electronics and wind power generators.